nature neuroscience

Directed differentiation of hippocampal stem/progenitor cells in the adult brain

Sebastian Jessberger[1,2], Nicolas Toni[1], Gregory D Clemenson Jr[1], Jasodhara Ray[1] & Fred H Gage[1]

Adult neurogenesis is a lifelong feature of brain plasticity; however, the potency of adult neural stem/progenitor cells *in vivo* remains unclear. We found that retrovirus-mediated overexpression of a single gene, the bHLH transcription factor Ascl1, redirected the fate of the proliferating adult hippocampal stem/progenitor (AHP) progeny and lead to the exclusive generation of cells of the oligodendrocytic lineage at the expense of newborn neurons, demonstrating that AHPs in the adult mouse brain are not irrevocably specified *in vivo*. These data indicate that AHPs have substantial plasticity, which might have important implications for the potential use of endogenous AHPs in neurological disease.

Adult neural stem cells continuously generate new neurons throughout adulthood in two distinct brain areas, the subventricular zone (SVZ) of the lateral ventricles and the subgranular zone (SGZ) of the dentate gyrus[1,2]. Newborn neurons go through distinct developmental steps, beginning with the division of a parental neural stem cell, before they become functionally integrated[3–5]. Adult neurogenesis appears to be critically involved in adult brain function and might also be involved in neurological disease[6,7]. Neural stem cells are cells that self-renew (reproducing themselves) and are multipotent (giving rise to all three neural lineages). Testing clonal self-renewal and multipotency requires the longitudinal observation of single stem cell behavior *in situ*[8], which is technically challenging in the adult brain. Thus, the evidence for self-renewal of neural stem cells in the adult brain is limited[9–12]. Furthermore, little conclusive data exist regarding the *in vivo* plastic capacity of adult neural stem cells[12], although previous reports have indicated that the neuronal fate of progenitors in the adult SVZ is plastic[13,14]. Most current concepts are based on or rely on data that were generated in the culture dish, under conditions that might differ markedly from the *in vivo* situation[15–18].

We sought to determine whether AHPs in their adult brain niche are capable of changing their fate. We directly tested this hypothesis using a retroviral strategy to label and genetically manipulate dividing cells and their progeny in the adult dentate gyrus. Notably, cell type–specific, retrovirus-mediated expression of Ascl1 (achaete-scute complex homolog-like 1, also known as Mash1) in AHPs redirected the fate of newborn cells from a neuronal to an oligodendrocytic lineage, indicating that the AHPs in the adult hippocampal niche retained fate plasticity.

RESULTS

Ascl1 redirects the fate of newborn cells

The majority of newborn cells were excitatory granule neurons 4 weeks after intrahippocampal injection of a retrovirus expressing green fluorescent protein (CAG-GFP). Most newborn cells showed the typical, highly polarized morphology of dentate granule cells and expressed the prospero-related homeobox 1 (Prox1) transcription factor and neuronal marker neuronal nuclei (NeuN, 85.7 ± 3.8%; **Fig. 1**). Only a very low number (2.5 ± 1.6%) of retrovirus-labeled cells colabeled with the oligodendrocytic marker NG2 4 weeks after virus injection, and we never observed newborn cells expressing later markers of the oligodendrocytic lineage, such as glutathione-S-transferase–π (GST-π), oligodendrocyte transcription factor 2 (Olig2), 2′,3′-cyclic nucleotide 3′-phosphodiesterase (CNPase) and myelin basic protein (MBP) under control conditions (**Fig. 1c** and **Supplementary Fig. 1** online)[19].

We next sought to challenge the fate plasticity of progenitors that appear to be mainly neurogenic under normal conditions to analyze the fate potential of AHPs *in vivo*. Retrovirus-mediated expression of Ascl1, which has been previously described to be involved in the generation of oligodendrocytes and GABAergic interneurons[20–22] in a context-dependent manner, markedly changed the morphology of newborn cells; they no longer colabeled for Prox1 and NeuN (**Fig. 1a**). Instead, cells transduced with the Ascl1-expressing retrovirus (CAG-Ascl1) exclusively colabeled with a distinct set of genes expressed in the oligodendrocytic lineage, such as NG2, GST-π and Olig2 (**Fig. 1b,c**)[19]. In contrast with newborn granule cells, which stay in the inner parts of the granule cell layer[23], a number of Ascl1-overexpressing cells migrated into the hilus (**Fig. 1a**), emphasizing the modified behavior of Ascl1-expressing cells compared with control cells.

Ascl1-induced cells differentiate into oligodendrocytes

Notably, a fraction of Ascl1-expressing cells showed coexpression of MBP (**Fig. 2a**) and CNPase (**Supplementary Fig. 2** online). MBP was found in the cytoplasm of Ascl1-expressing cells and in thin processes

[1]Laboratory of Genetics, The Salk Institute for Biological Studies, 10010 N. Torrey Pines Road, La Jolla, California 92037, USA. [2]Institute of Cell Biology, Department of Biology, Swiss Federal Institute of Technology (ETH) Zurich, Schafmattstrasse 18, 8093 Zurich, Switzerland. Correspondence should be addressed to F.H.G. (gage@salk.edu) or S.J. (jessberger@cell.biol.ethz.ch).

Received 18 January; accepted 23 May; published online 29 June 2008; doi:10.1038/nn.2148

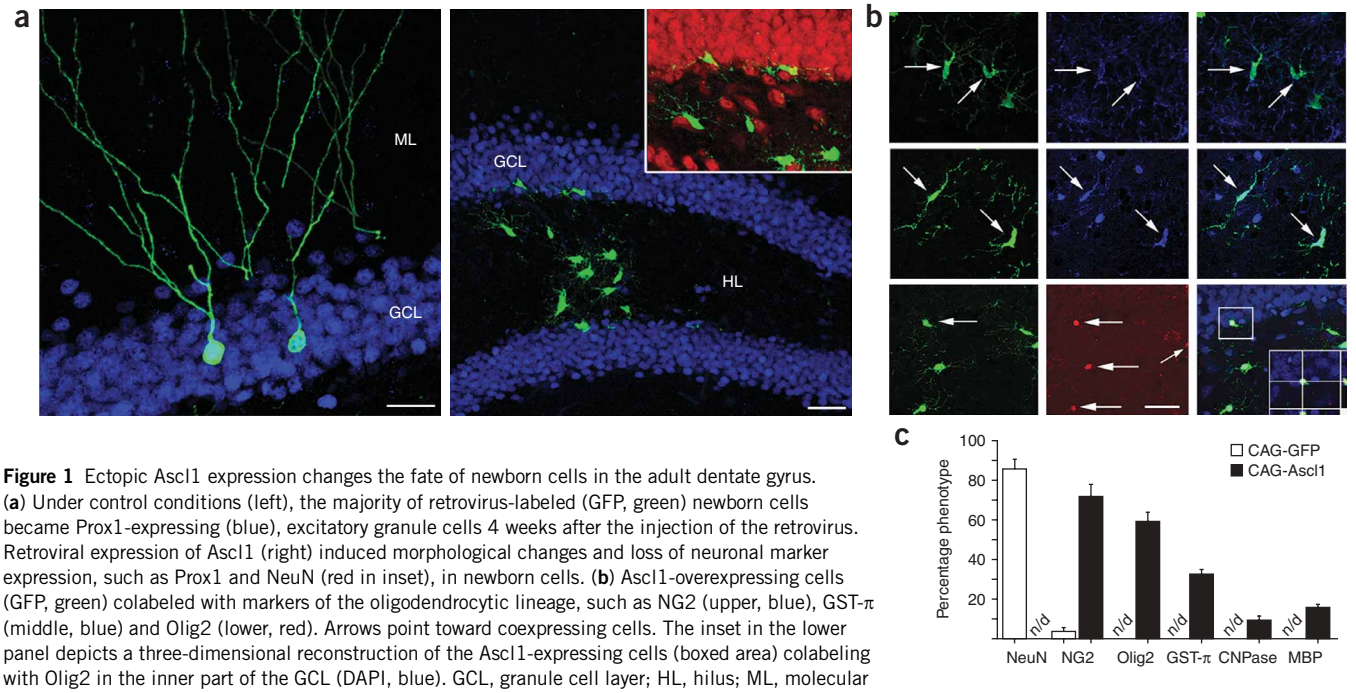

Figure 1 Ectopic Ascl1 expression changes the fate of newborn cells in the adult dentate gyrus. (**a**) Under control conditions (left), the majority of retrovirus-labeled (GFP, green) newborn cells became Prox1-expressing (blue), excitatory granule cells 4 weeks after the injection of the retrovirus. Retroviral expression of Ascl1 (right) induced morphological changes and loss of neuronal marker expression, such as Prox1 and NeuN (red in inset), in newborn cells. (**b**) Ascl1-overexpressing cells (GFP, green) colabeled with markers of the oligodendrocytic lineage, such as NG2 (upper, blue), GST-π (middle, blue) and Olig2 (lower, red). Arrows point toward coexpressing cells. The inset in the lower panel depicts a three-dimensional reconstruction of the Ascl1-expressing cells (boxed area) colabeling with Olig2 in the inner part of the GCL (DAPI, blue). GCL, granule cell layer; HL, hilus; ML, molecular layer. (**c**) Quantification of newborn cells 4 weeks after injection of CAG-GFP or CAG-Ascl1 resulted in the complete loss of newborn neurons (expressing NeuN) following CAG-Ascl1 injection and the subsequent conversion of AHPs to NG2- (69.7 ± 5.2%), GST-π– (31.8 ± 2.4), Olig2- (59.8 ± 5.1%), CNPase- (9.9 ± 3.2%) and MBP-expressing (16.0 ± 2.1%) cells. Note that these numbers do not add up to 100%, as subsequent stainings were required because of species overlap of the antibodies that we used. Error bars represent s.e.m. Scale bars represent 50 μm.

that wrapped or followed neurofilament heavy chain (NF200kd)-expressing axons (**Fig. 2a–c**), suggesting that a fraction of AHP-derived oligodendrocytic cells might have the potential to myelinate[24]. Supporting a gradual maturation process of Ascl1-expressing cells, we analyzed the expression pattern of NG2 and MBP at several time points after viral injection and found a decrease in NG2 colabeling over time, whereas MBP expression increased with the age of newborn cells (percentage of coexpression with Ascl1-expressing cells at 4 d, 14 d and 4 weeks; NG2: 91.6 ± 5.7%, 78.2 ± 3.7% and 69.7 ± 5.2%; MBP: not detected, 7.1 ± 2.2% and 16.0 ± 2.1%).

To obtain independent ultrastructural evidence that Ascl1-expressing cells had indeed changed their fate, we analyzed GFP-positive cells at the electron-microscopic level using pre-embedding immunostaining and serial sectioning. We observed several morphological characteristics of oligodendrocyte or oligodendrocyte precursor cells, such as a clumpy chromatin, a large oval nucleus occupying most of the cell body, a cytoplasm lying in an eccentric position and containing numerous vesicular bodies, including a large Golgi apparatus, and several myelinated fibers in close vicinity to the cell body (**Fig. 2d**). Thus, the ultrastructural characteristics, whole-cell morphology and observed switch in marker expression indicated that retroviral Ascl1 expression changed the fate of AHP progeny from a neuronal to an oligodendrocytic phenotype.

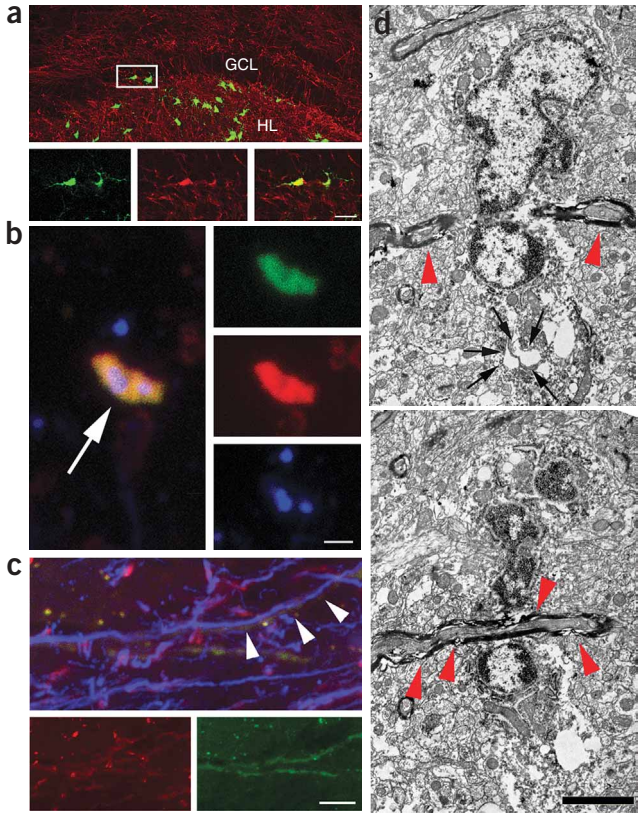

Figure 2 Ascl1-expressing newborn cells have features of myelinating oligodendrocytes. (**a**) A population of Ascl1-overexpressing cells (GFP, green) colabeled with MBP (red) expressed in the cytoplasm. Insets show high-power views of the boxed area. (**b**,**c**) MBP-labeled processes (red) extending from Ascl1-overexpressing cells (GFP, green) seemed to wrap around (arrow in **b**) or follow along (arrowheads in **c**) axons (NF200kd, blue) in the hilus (**b**) or the SGZ (**c**). (**d**) Serial-section electron microscopy of CAG-Ascl1–labeled cell revealed characteristics of oligodendrocyte or oligodendrocyte precursor cells; that is, heterochromatin, large nucleus, a large Golgi apparatus (arrows) and several myelinated fibers close to the cell body (red arrowheads), supporting the oligodendrocytic fate of newborn, Ascl1-overexpressing cells. Shown are two sections of the same cell at different *z* levels. Scale bars represent 40 μm in **a** and 2 μm in **b**–**d**.

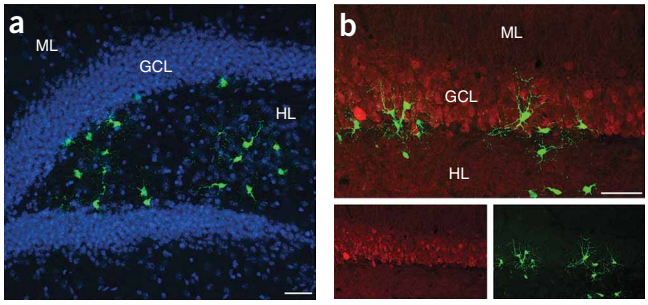

Figure 3 Long-term survival and species consistency of Ascl1-expressing cells. (**a**) Newborn CAG-Ascl1–transduced cells (GFP, green) survived for at least 3 months following virus injection into the adult dentate gyrus (nuclei visualized with DAPI, blue). (**b**) The fate-directing effect of CAG-Ascl1 was conserved between species, as CAG-Ascl1 injection also changed the fate of newborn cells (GFP, green) in the dentate gyrus of adult rats that lost the coexpression with Ca^{2+}-binding calbindin (red). Scale bars represent 50 μm.

Notably, Ascl1-induced oligodendrocytic cells became stably integrated into the dentate area and could be detected 3 months after virus injection (**Fig. 3a**). The effect of Ascl1 overexpression on the fate of AHP progeny was also consistent between species; we found a conversion from neurogenic to oligodendrogenic AHPs in the hippocampus of adult rats (**Fig. 3b**).

Ascl1-expressing virus targets neurogenic AHPs

The generation of oligodendrocytic cells occurred at the complete expense of granule cells, indicating the directed fate change of AHPs that predominantly give rise to neurons under normal conditions (**Fig. 1c**). We used several independent strategies to show that AHPs that are neurogenic under control conditions indeed changed their fate with Ascl1 induction. Time course analysis showed that Ascl1-expressing and control virus–transduced AHPs were indistinguishable 24 h after virus injection (**Fig. 4a**,**b**). We did not find any cells expressing NG2 at that time point, but the number of cells expressing the SRY-related HMG-box gene 2 (Sox2)[25] or doublecortin (DCX)[26] did not significantly differ ($P > 0.4$) between control and Ascl1-expressing cells (**Fig. 4b**). However, 4 d after injection, control cells colabeled with the immature neuronal marker DCX, whereas Ascl1-expressing cells colabeled with NG2. The divergence between control and Ascl1-expressing cells became even more evident 14 d after injection; control cells extended dendritic processes into the molecular layer, whereas many Ascl1-expressing cells had migrated into the polymorphic cell layer (**Fig. 4a**). We next asked whether there were differences in viral tropism between CAG-GFP and CAG-Ascl1 viruses. We co-injected CAG-Ascl1 retrovirus with RFP-expressing control virus and found that Ascl1-targeted cells were also transduced with the RFP virus (**Fig. 4c**). Quantification of single- and colabeled cells showed that the relative number of cells labeled only with the RFP virus was unchanged when Ascl1-expressing virus was co-injected when compared with co-injections of GFP control virus with RFP virus (**Supplementary Fig. 3** online). This finding suggests that the viral transduction with the Ascl1-expressing virus occurred in the same cell population that was also transduced with the RFP-expressing control virus.

We found no differences in the numbers of apoptotic cells labeled with control virus or Ascl1-expressing virus using activated caspase-3 labeling (data not shown); a rise in the number of apoptotic cells would be expected if Ascl1 expression simply killed all neurogenic cells and at the same time expanded and differentiated oligodendrocytic precursors. In addition, all Ascl1-induced cells and control cells were postmitotic 4 weeks after viral injection, as we found no coexpression of virus labeled with the cell cycle–associated protein Ki67 at this time point (data not shown).

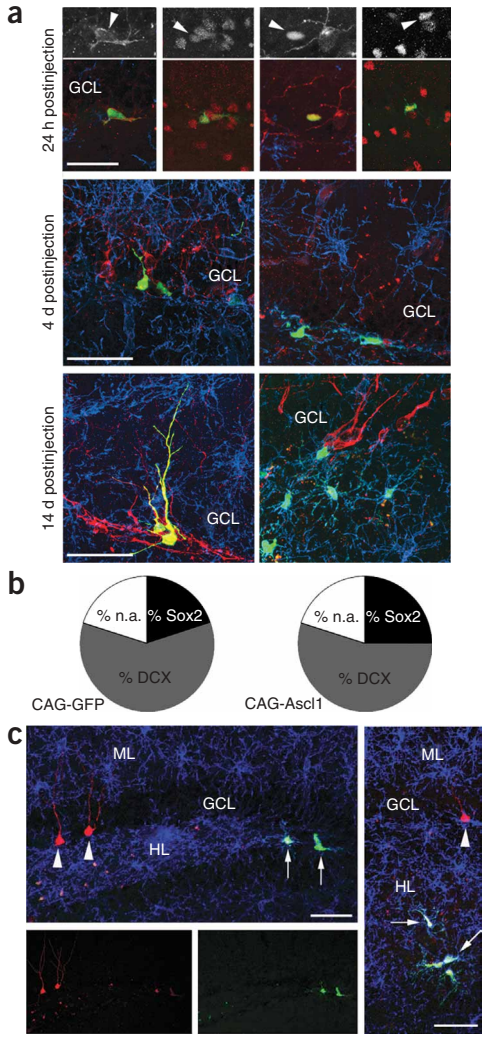

Figure 4 Progeny of Ascl1-overexpressing cells and cells born under control conditions share common AHPs. (**a**,**b**) Time course experiments showed that cells transduced with CAG-GFP (green, left) were indistinguishable from CAG-Ascl1–transduced cells (green, right) 24 h after virus injection and commonly expressed DCX (red in first and third upper panel) and Sox2 (red in second and fourth upper panel), but not NG2 (blue, upper). Insets show single channels for DCX and Sox2. The percentages of cells expressing NG2, DCX or neither of the two markers (n.a.), 24 h following CAG-GFP and CAG-Ascl1 injection are shown in **b**. Control cells (GFP, green) started to extend apical dendrites and express DCX (red) 4 d after virus injection, whereas Ascl1-overexpressing cells (GFP, green) colabeled with NG2, but were still mostly localized in the SGZ (middle). Dendrites of control cells (DCX, red) reached the distal molecular layer by 14 d after injection, whereas Ascl1-overexpressing cells still colabeled with NG2 (blue) and started to migrate into the hilus. (**c**) Injection of CAG-RFP control virus together with CAG-Ascl1 and subsequent colabeling in newborn cells 4 weeks after virus injection further confirmed the targeting of common AHPs. Note that exclusively RFP-only transduced cells (arrowheads) became granule cells, whereas all cotransduced cells (arrows) showed an oligodendrocytic morphology and partially expressed NG2 (blue). Shown are two examples. Scale bars represent 50 μm.

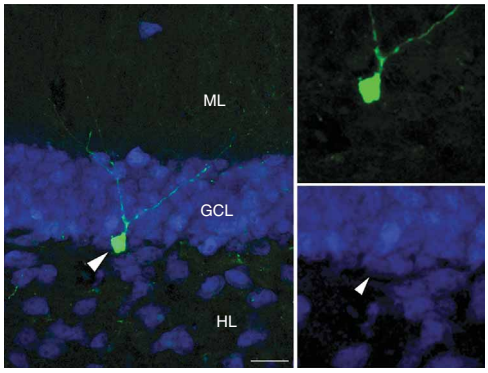

Figure 5 Retroviral Dlx2 does not affect neuronal differentiation in the adult hippocampus. Newborn cells that were transduced with a Dlx2-expressing retrovirus (GFP, green) differentiated into NeuN-expressing granule cells (blue, arrowhead in the lower right points toward the GFP-expressing colabeled cell). Note the typical granule-cell morphology with an apical dendrite extending into the molecular layer 2 weeks after viral injection. Scale bar represents 20 μm.

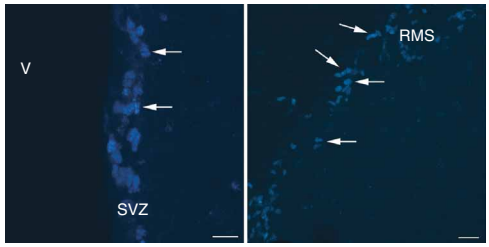

Figure 6 Ascl1 is expressed in the adult SVZ and rostral migratory stream (RMS). Arrows point to cells expressing high levels of Ascl1 (blue) detected in the SVZ (left panel) and in the RMS (right panel) of adult mice. In contrast, we found no expression of Ascl1 in the adult dentate gyrus under the exact same staining conditions and using tissue from the same animals. V, ventricle. Scale bars represent 50 μm.

The ability of AHPs that are mostly neurogenic under normal conditions to adopt an oligodendrocytic fate with Ascl1 expression is supported by previous studies showing that oligodendrocytes and neurons can share a common progenitor, both during embryonic development and in the adult brain[14,27]. We found it interesting that the effects of Ascl1 on neural fate decision were not dependent on *Dlx* gene expression[28], as overexpression of *Dlx1*, *Dlx2* and *Dlx5* did not alter the neuronal fate of AHPs (**Fig. 5** and data not shown).

Context-dependent effects of Ascl1 expression

To analyze a potential context-dependent effect of Ascl1 (ref. 20) in the adult brain, we injected Ascl1-expressing retrovirus into the SVZ of the lateral ventricles. Although the Ascl1 promoter appears to be active in hippocampal type 2 progenitor cells[29], we only found protein expression of Ascl1 in the adult SVZ, and not in the adult hippocampus (**Fig. 6** and data not shown), suggesting that Ascl1 function and importance might be substantially different in the adult SVZ and in the context of neuronal differentiation of dentate granule cells. Indeed, retroviral Ascl1 expression in the SVZ did not induce a fate switch and neuronal differentiation of olfactory neurons was not substantially affected (**Fig. 7a**).

We next sought to determine whether the obvious differences in Ascl1 action in the dentate gyrus and SVZ are maintained if AHPs are isolated and propagated *in vitro*. To this end, we isolated multipotent progenitors specifically from the dentate gyrus of adult rats (**Supplementary Fig. 4** online). In marked contrast to the *in vivo* effects, Ascl1 overexpression potently induced neuronal differentiation of AHPs *in vitro* (Tuj1, 82.3 ± 6.2%; MAP2ab, 71.8 ± 5.6%; colabeled cells) compared with AHPs labeled with a control virus (Tuj1, 2.1 ± 1.3%; MAP2ab, 1.7 ± 0.9%; $P < 0.001$) (**Fig. 7b**), similar to the effect of Ascl1 overexpression on SVZ progenitors (**Supplementary Fig. 4**). This finding highlights the context-dependent effects of Ascl1 and indicates that unknown local environmental clues in the adult dentate gyrus instruct AHPs to adopt an oligodendroytic fate on Ascl1 transduction.

DISCUSSION

We show here that AHPs can be instructed by expression of a single gene to differentiate into different neural fates in their *in vivo* niche. Thus, our data demonstrate the fate plasticity of AHPs in the adult brain.

Ascl1 is a bHLH transcription factor that has previously been implicated in the generation of oligodendrocytes and GABAergic interneurons during embryonic and early postnatal development[20–22]. Consistent with earlier studies, we found high levels of Ascl1 expression in the SVZ, suggesting that Ascl1 is involved in the generation of at least some types of olfactory neurons that are generated throughout life[20,29]. Retrovirus-mediated Ascl1 overexpression in the SVZ did not result in substantial alterations of olfactory neurogenesis, supporting the idea that Ascl1 has a physiological role in olfactory neurogenesis. In marked contrast to findings in the SVZ, we found no substantial levels of Ascl1 protein expression in the adult hippocampus, even though the endogenous Ascl1 promoter appears to be active in distinct sets of

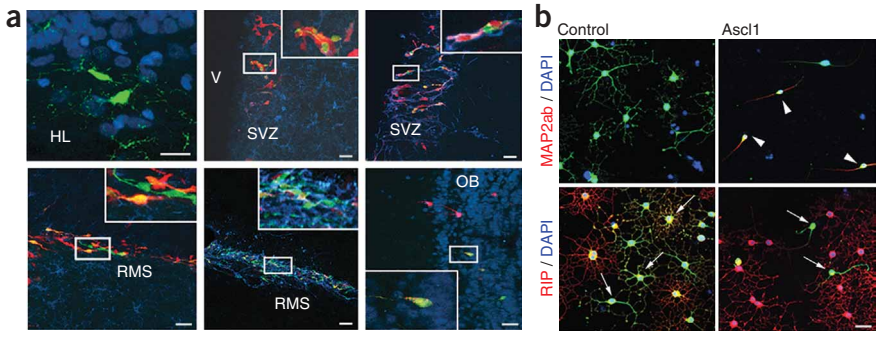

Figure 7 Context-dependent effects of Ascl1. (**a**) In contrast with the dentate gyrus, where Ascl1 expression induced the generation of oligodendroytic cells (green, upper left) at the expense of new neurons (NeuN in blue), Ascl1-expressing cells (green, upper middle) in the SVZ were comparable to cells labeled with control virus CAG-RFP (red) 1 week after viral injection and did not express NG2 (blue, upper middle), but colabeled with DCX (blue, upper right). There were also no morphological differences between Ascl1- and RFP-expressing newborn cells in the RMS, where Ascl1- and RFP-expressing cells did not colabel with NG2 (lower left) but did colabel with DCX (lower middle). Ascl1-expressing cells in the olfactory bulb were not distinguishable from RFP-expressing newborn olfactory neurons (NeuN in blue, lower right) 4 weeks after viral injection. Insets show high-power views of the boxed areas. (**b**) Ascl1 induced neuronal differentiation (MAP2ab in red, upper) when retrovirally overexpressed in AHPs *in vitro* compared with control cells and prevented spontaneous oligodendrocytic differentiation (RIP in red, lower). OB, olfactory bulb. Scale bars represent 20 μm.

AHPs[29]. However, Ascl1 seems to be dispensable for hippocampal granule cell development, at least during embryonic stages[30], which is in contrast with other bHLH transcription factors, such as NeuroD1 and neurogenin-2 (refs. 30–32).

Given the extensively described role for Ascl1 in oligodendrocytic development[33–36], we hypothesized that cell type–specific expression of Ascl1 in AHPs might redirect the fate of their progeny. Indeed, retrovirus-mediated expression of Ascl1 instructed AHPs to generate cells of the oligodendrocytic lineage rather than generate excitatory granule cells, which is the predominant phenotype generated under normal conditions. This effect was strongly dependent on the cellular context, as AHPs (showing unambiguous multipotency *in vitro*) differentiated into neuronal cells when transduced with Ascl1-expressing retrovirus in the culture dish, suggesting distinct features of AHPs in their dentate gyrus niche compared with *in vitro* conditions.

AHPs are multipotent *in vitro*[16,18,37,38], but the fate potential of AHPs remains unknown. Our data clearly show that AHPs retain the potential to switch fate even in the adult hippocampus. A recent study suggested that neural stem cells derived from the SVZ show a region-specific diversity that is also maintained on heterotopic transplantation[39]. These findings point toward neural stem cell diversity between or even within neurogenic areas of the adult brain. However, our results show that restrictions in fate plasticity of neural stem cells in a niche are not definite and can be overcome. This finding has potential clinical relevance, as many neurological diseases, such as multiple sclerosis, stroke and epilepsy, not only affect neuronal cells, but also disrupt the functioning of other neural cell types, such as oligodendrocytes[40–42]. Thus, the finding that the fate of AHPs can be respecified by a single gene has implications for endogenous brain repair.

METHODS

Plasmids and retroviruses. Expression constructs of Ascl1 (a gift from K. Nakashima, Nara Institute of Science and Technology), Dlx1, Dlx2 and Dlx5 (gifts from J.L.R. Rubenstein, University of California, San Francisco) were subcloned into a Moloney murine leukemia retrovirus in which the expression of the transgene is driven by the compound promoter CAG, containing the CMV enhancer/chicken β-actin promoter and a large synthetic intron, as well as an IRES-GFP (a gift from I. Verma, Salk Institute of Biological Studies). Control viruses expressed GFP (CAG-GFP) or mRFP (CAG-RFP; mRFP construct was a gift from R.Y. Tsien, University of California, San Diego) under the same promoter. Retroviruses were produced as described earlier[43] and titers ranged between 2.5 and 5 × 10^7 cfu ml^{-1}.

Immunostaining. Tissue and cells were fixed and processed for immunostaining as described earlier[44]. As primary antibodies, we used rabbit antibody to GFP (Molecular Probes), chicken antibody to GFP (Aves), rabbit antibody to Prox1 (Chemicon), rabbit antibody to Sox2 (Chemicon), mouse antibody to NeuN (Chemicon), goat antibody to DCX (Santa Cruz), mouse antibody to GST-π (BD Pharmingen), rat antibody to MBP (Serotec), rabbit antibody to NG2 (Chemicon), rabbit antibody to NF200kd (Chemicon), mouse antibody to Ascl1 (BD Pharmingen), rabbit antibody to Olig2 (Chemicon), mouse antibody to MAP2ab (Sigma), rabbit antibody to Tuj1 (Covance), mouse antibody to CNPase (Covance), mouse antibody to RIP (Hybridoma Bank), guinea pig antibody to GFAP (Advanced ImmunChemical), mouse antibody to calbindin (Swant), goat antibody to DCX (Santa Cruz) and rabbit antibody to Ki67 (Vector Laboratories). Secondary antibodies were obtained from the Jackson Laboratory.

Animals and retrovirus injections. Animal procedures were performed in accordance with protocols approved by the Institutional Animal Care Use Committee of the Salk Institute for Biological Studies. All mice used in this study were 8–11-week-old female C57Bl/6 mice (purchased from Harlan or Livermore). Mice were stereotactically injected with 1 μl of the CAG-GFP–, CAG-Ascl1– or CAG-RFP–expressing viruses, or 1.5 μl of 1:1 mixtures of CAG-GFP/CAG-RFP– and CAG-Ascl1/CAG-RFP–expressing viruses into the dentate gyrus (coordinates from bregma were –2 anterior/posterior, ±1.5 medial/lateral and –2.3 dorsal/ventral from skull). For the experiments in the SVZ, animals were injected with a 1:1 mixture of CAG-GFP/CAG-RFP– and CAG-Ascl1/CAG-RFP–expressing viruses (coordinates from bregma were –1 anterior/posterior, –1.0 medial/lateral and –2.8 dorsal/ventral from skull). Animals were transcardially perfused at the respective time points (group sizes, $n = 3$). To phenotype virus-labeled cells, all GFP-expressing cells were analyzed for the expression of NeuN or oligodendrocytic markers (NG2, GST-π, MBP, Olig2 and CNPase) in separate stainings throughout the rostro-caudal extent of the dentate gyrus using a 1-in-6 series. To analyze the ratio of colabeled cells following injection of viral mixtures, we counted all virus-labeled cells again using a 1-in-6 series and formed a ratio between GFP- and RFP-expressing cells. To analyze the phenotype of virus-labeled cells 24 h, 4 d and 14 days after injection, we counted for each time point at least 20 CAG-GFP– and 20 CAG–Ascl1-expressing cells.

Statistical analysis. All statistical analyses were carried out using Statview 5.0.1 (SAS). For all comparisons, ANOVA was performed, followed by Fisher's *post hoc* test when appropriate. Differences were considered to be statistically significant at $P < 0.05$.

Adult stem/progenitor cell cultures. The dentate gyrus and the SVZ of adult female rats were dissected, and progenitors were isolated and propagated as described previously[16,45]. To determine multipotency, we treated AHPs with retinoic acid/forskolin, BMP-1/LIF or IGF-1 (refs. 44,46). AHPs were transduced with Ascl1- or CAG-GFP–expressing retrovirus, transferred into medium containing DMEM:F12/N2 (Sigma) without FGF-2 (ref. 16) and fixed 5 d after transduction. Immunostaining was carried out as described previously[44].

Electron microscopy. Mice were transcardially perfused with 4% paraformaldehyde (wt/vol) in 0.1 M phosphate buffer, pH 7.4, at room temperature (20 ± 3 °C) for 10 min. The brain was removed 15 h after the perfusion was stopped and was postfixed for 48 h in 4% paraformaldehyde. We cut 50-μm horizontal vibratome sections, cryoprotected them in 2% glycerol and 20% DMSO (vol/vol) in 0.1 M phosphate buffer for 20 min and freeze/thawed the sections eight times in liquid nitrogen. After a treatment in 0.3% hydrogen peroxide (vol/vol, five times for 5 min each) and three 10-min washes in phosphate buffer with 0.5% bovine serum albumin (vol/vol, BSA-C, Aurion), slices were incubated overnight in the primary antibody (rabbit antibody to GFP, Chemicon) in phosphate buffer with 0.1% BSA-C at 4 °C. After washing in phosphate buffer with 0.1% BSA-C, the sections were incubated for 4 h at room temperature (20 ± 3 °C) in biotinylated secondary antibody (goat antibody to rabbit, Jackson Laboratories). To reveal this labeling, we incubated slices for 2 h in avidin biotin peroxidase complex (ABC Elite, Vector Laboratories), followed by 3,3′-diaminobenzidine tetrachloride (Vector Laboratories Kit) for 10–20 min. The sections were then postfixed overnight in 2.5% glutaraldehyde (vol/vol), washed in 0.1 M phosphate buffer, postfixed in osmium tetroxide for 1 h, dehydrated and embedded in Epoxy resin.

Serial sections were cut at 40-nm thickness, collected on single-slot grids and contrasted by incubating for 35 min in 5% uranyl acetate solution (wt/vol), followed by 25 min in Reynolds solution. Serial images of the labeled structures were then collected with a digital camera (MegaView III, SIS) mounted on a JEOL 100 CXII transmission electron microscope at a 19,000× magnification with a filament voltage of 80 kV.

Note: Supplementary information is available on the Nature Neuroscience website.

ACKNOWLEDGMENTS

We thank M.L. Gage for editing the manuscript. The study was supported by grants from the Deutsche Forschungsgemeinschaft (Je297/1-1), American Epilepsy Society, Swiss National Science Foundation (to S.J.), and the US National Institute on Aging, the US National Institute of Neurological Disorders and Stroke, the Lookout Fund, the Christopher and Dana Reeve Foundation, the Picower Foundation and Project ALS (to F.H.G.).

AUTHOR CONTRIBUTIONS

S.J. conceived and carried out the experiments, analyzed the data and wrote the manuscript. N.T. performed the electron microscopy experiment. G.D.C.

participated in viral injections and histological procedures. J.R. provided the stem cell cultures. F.H.G. revised the manuscript, gave conceptual input and obtained financial support.

Published online at http://www.nature.com/natureneuroscience/
Reprints and permissions information is available online at http://npg.nature.com/reprintsandpermissions/

1. Gage, F. Mammalian neural stem cells. *Science* **287**, 1433–1438 (2000).
2. Alvarez-Buylla, A. & Lim, D.A. For the long run: maintaining germinal niches in the adult brain. *Neuron* **41**, 683–686 (2004).
3. van Praag, H. *et al.* Functional neurogenesis in the adult hippocampus. *Nature* **415**, 1030–1034 (2002).
4. Ge, S., Yang, C.H., Hsu, K.S., Ming, G.L. & Song, H. A critical period for enhanced synaptic plasticity in newly generated neurons of the adult brain. *Neuron* **54**, 559–566 (2007).
5. Carleton, A., Petreanu, L.T., Lansford, R., Alvarez-Buylla, A. & Lledo, P.M. Becoming a new neuron in the adult olfactory bulb. *Nat. Neurosci.* **6**, 507–518 (2003).
6. Sahay, A. & Hen, R. Adult hippocampal neurogenesis in depression. *Nat. Neurosci.* **10**, 1110–1115 (2007).
7. Zhao, C., Deng, W. & Gage, F.H. Mechanisms and functional implications of adult neurogenesis. *Cell* **132**, 645–660 (2008).
8. Noctor, S.C., Flint, A.C., Weissman, T.A., Dammerman, R.S. & Kriegstein, A.R. Neurons derived from radial glial cells establish radial units in neocortex. *Nature* **409**, 714–720 (2001).
9. Ahn, S. & Joyner, A.L. *In vivo* analysis of quiescent adult neural stem cells responding to Sonic hedgehog. *Nature* **437**, 894–897 (2005).
10. Doetsch, F., Caille, I., Lim, D.A., Garcia-Verdugo, J.M. & Alvarez-Buylla, A. Subventricular zone astrocytes are neural stem cells in the adult mammalian brain. *Cell* **97**, 703–716 (1999).
11. Consiglio, A. *et al.* Robust *in vivo* gene transfer into adult mammalian neural stem cells by lentiviral vectors. *Proc. Natl. Acad. Sci. USA* **101**, 14835–14840 (2004).
12. Suh, H. *et al. In vivo* fate analysis reveals the multipotent and self-renewal capacities of Sox2(+) neural stem cells in the adult Hippocampus. *Cell Stem Cell* **1**, 515–528 (2007).
13. Hack, M.A. *et al.* Neuronal fate determinants of adult olfactory bulb neurogenesis. *Nat. Neurosci.* **8**, 865–872 (2005).
14. Jackson, E.L. *et al.* PDGFRα-positive B cells are neural stem cells in the adult SVZ that form glioma-like growths in response to increased PDGF signaling. *Neuron* **51**, 187–199 (2006).
15. Gabay, L., Lowell, S., Rubin, L.L. & Anderson, D.J. Deregulation of dorsoventral patterning by FGF confers trilineage differentiation capacity on CNS stem cells *in vitro*. *Neuron* **40**, 485–499 (2003).
16. Ray, J. & Gage, F.H. Differential properties of adult rat and mouse brain-derived neural stem/progenitor cells. *Mol. Cell. Neurosci.* **31**, 560–573 (2006).
17. Seaberg, R.M. & van der Kooy, D. Adult rodent neurogenic regions: the ventricular subependyma contains neural stem cells, but the dentate gyrus contains restricted progenitors. *J. Neurosci.* **22**, 1784–1793 (2002).
18. Bull, N.D. & Bartlett, P.F. The adult mouse hippocampal progenitor is neurogenic, but not a stem cell. *J. Neurosci.* **25**, 10815–10821 (2005).
19. Rowitch, D.H. Glial specification in the vertebrate neural tube. *Nat. Rev. Neurosci.* **5**, 409–419 (2004).
20. Parras, C.M. *et al.* Mash1 specifies neurons and oligodendrocytes in the postnatal brain. *EMBO J.* **23**, 4495–4505 (2004).
21. Battiste, J. *et al.* Ascl1 defines sequentially generated lineage-restricted neuronal and oligodendrocyte precursor cells in the spinal cord. *Development* **134**, 285–293 (2007).
22. Petryniak, M.A., Potter, G.B., Rowitch, D.H. & Rubenstein, J.L. Dlx1 and Dlx2 control neuronal versus oligodendroglial cell fate acquisition in the developing forebrain. *Neuron* **55**, 417–433 (2007).
23. Duan, X. *et al.* Disrupted-In-Schizophrenia 1 regulates integration of newly generated neurons in the adult brain. *Cell* **130**, 1146–1158 (2007).
24. Sherman, D.L. & Brophy, P.J. Mechanisms of axon ensheathment and myelin growth. *Nat. Rev. Neurosci.* **6**, 683–690 (2005).
25. Avilion, A.A. *et al.* Multipotent cell lineages in early mouse development depend on SOX2 function. *Genes Dev.* **17**, 126–140 (2003).
26. Couillard-Despres, S. *et al.* Doublecortin expression levels in adult brain reflect neurogenesis. *Eur. J. Neurosci.* **21**, 1–14 (2005).
27. Lu, Q.R. *et al.* Common developmental requirement for Olig function indicates a motor neuron/oligodendrocyte connection. *Cell* **109**, 75–86 (2002).
28. Poitras, L., Ghanem, N., Hatch, G. & Ekker, M. The proneural determinant MASH1 regulates forebrain Dlx1/2 expression through the I12b intergenic enhancer. *Development* **134**, 1755–1765 (2007).
29. Kim, E.J., Leung, C.T., Reed, R.R. & Johnson, J.E. *In vivo* analysis of Ascl1 defined progenitors reveals distinct developmental dynamics during adult neurogenesis and gliogenesis. *J. Neurosci.* **27**, 12764–12774 (2007).
30. Galichet, C., Guillemot, F. & Parras, C.M. Neurogenin 2 has an essential role in development of the dentate gyrus. *Development* **135**, 2031–2041 (2008).
31. Liu, M. *et al.* Loss of β2/NeuroD leads to malformation of the dentate gyrus and epilepsy. *Proc. Natl. Acad. Sci. USA* **97**, 865–870 (2000).
32. Miyata, T., Maeda, T. & Lee, J.E. NeuroD is required for differentiation of the granule cells in the cerebellum and hippocampus. *Genes Dev.* **13**, 1647–1652 (1999).
33. Kondo, T. & Raff, M. Basic helix-loop-helix proteins and the timing of oligodendrocyte differentiation. *Development* **127**, 2989–2998 (2000).
34. Sugimori, M. *et al.* Ascl1 is required for oligodendrocyte development in the spinal cord. *Development* **135**, 1271–1281 (2008).
35. Sugimori, M. *et al.* Combinatorial actions of patterning and HLH transcription factors in the spatiotemporal control of neurogenesis and gliogenesis in the developing spinal cord. *Development* **134**, 1617–1629 (2007).
36. Parras, C.M. *et al.* The proneural gene Mash1 specifies an early population of telencephalic oligodendrocytes. *J. Neurosci.* **27**, 4233–4242 (2007).
37. Babu, H., Cheung, G., Kettenmann, H., Palmer, T.D. & Kempermann, G. Enriched monolayer precursor cell cultures from micro-dissected adult mouse dentate gyrus yield functional granule cell-like neurons. *PLoS ONE* **2**, e388 (2007).
38. Palmer, T.D., Ray, J. & Gage, F.H. FGF-2–responsive neuronal progenitors reside in proliferative and quiescent regions of the adult rodent brain. *Mol. Cell. Neurosci.* **6**, 474–486 (1995).
39. Merkle, F.T., Mirzadeh, Z. & Alvarez-Buylla, A. Mosaic organization of neural stem cells in the adult brain. *Science* **317**, 381–384 (2007).
40. Pitt, D., Werner, P. & Raine, C.S. Glutamate excitotoxicity in a model of multiple sclerosis. *Nat. Med.* **6**, 67–70 (2000).
41. Sperk, G. *et al.* Kainic acid–induced seizures: neurochemical and histopathological changes. *Neuroscience* **10**, 1301–1315 (1983).
42. Back, S.A. *et al.* Selective vulnerability of late oligodendrocyte progenitors to hypoxia-ischemia. *J. Neurosci.* **22**, 455–463 (2002).
43. Zhao, C., Teng, E.M., Summers, R.G. Jr, Ming, G.L. & Gage, F.H. Distinct morphological stages of dentate granule neuron maturation in the adult mouse hippocampus. *J. Neurosci.* **26**, 3–11 (2006).
44. Lie, D.C. *et al.* Wnt signaling regulates adult hippocampal neurogenesis. *Nature* **437**, 1370–1375 (2005).
45. Lein, E.S., Zhao, X. & Gage, F.H. Defining a molecular atlas of the hippocampus using DNA microarrays and high-throughput *in situ* hybridization. *J. Neurosci.* **24**, 3879–3889 (2004).
46. Hsieh, J. *et al.* IGF-I instructs multipotent adult neural progenitor cells to become oligodendrocytes. *J. Cell Biol.* **164**, 111–122 (2004).